3

Periodically Poled Acoustic Wave-Guide and Transducers for Radio-Frequency Applications

Sylvain Ballandras et al.*
FEMTO-ST, UMR 6174 CNRS-UFC-ENSMM-UTBM, Time&Frequency Dept,
**PHOTLINE Technologies,*
France

1. Introduction

The demand for highly coupled high quality acoustic wave devices for RF signal processing based on passive devices has generated a strong innovative activity, yielding the investigation of new excitation principles and waveguide structures. Among all the tested devices, one can mention thick passivation SiO_2-based structures using high velocity modes on lithium niobate ($LiNbO_3$) or lithium tantalate ($LiTaO_3$) (Kando et al, 2006), (Gachon et al. 2010), yielding the definition of interface or isolated-wave-based devices but modes excited on compound substrates (Elmazria et al, 2009), for instance consisting of a piezoelectric layer (AlN, ZnO, single crystal $LiNbO_3$ or $LiTaO_3$, etc.) deposited atop a high acoustic wave velocity material such as diamond-C, silicon carbide, sapphire, silicon, and so on (Higaki et al, 1997), (Iriarte et al, 2003), (Salut & al, 2010). All these devices generally exploit inter-digitized transducers (IDTs) operating at Bragg frequency (Morgan, 1985), i.e. exhibiting a mechanical period equal to a half-wavelength of the acoustic propagation. Although passivation allows for an improved power handling compared to IDTS on free surfaces, this feature is still limited by electro-migration and material diffusion phenomena (Greer et al, 1990). An interesting answer to this problem is the use of bulk acoustic waves in thin films exhibiting a high disruptive field material such as AlN (Lakin, 2003), (Lanz, 2005). In that case, the frequency control reveals more difficult than for IDT based devices, as the resonance frequency of the so-called Film Bulk Acoustic Resonators (FBARs) is proportional to the film thickness. As significant progresses were achieved in thin film technologies during the last decade, this did not prevent the use of FBARs for actual low-loss RF filter implementation (Bradley et al, 2000). Nevertheless, it turns out there is still missing capabilities for better controlling the operation frequency of these passive devices, particularly for future generations of telecommunication systems which push toward higher RF bands than those exploited until now.

The idea to transfer the transducer periodicity within the substrate has been shared by numerous scientists but it took rather a long term before the first experimental evidence, allowing for a correlation between theory and experiment and hence yielding a satisfying explanation of the corresponding mode distribution and realistic property description.

* Emilie Courjon, Florent Bassignot, Gwenn Ulliac, *Jérôme Hauden, Julien Garcia, Thierry Laroche and William Daniau

Although our very first proof of concept were built on a PZT substrate (Ballandras et al 2003) and after on an epitaxial PZT thin film grown on $SrTiO_3$ (Sarin Kumar et al, 2004), the first convincing experiments were performed on 500µm thick 3" $LiNbO_3$ Z-cut wafers of optical quality answering severe specifications on total thickness variation and side parallelism (Courjon et al, 2007). The fabrication of periodically poled transducers (PPTs) on such wafers has allowed for the excitation of symmetrical Lamb modes with an operating frequency twice higher than those obtained using standard inter-digitized transducers. The corresponding devices have been successfully manufactured and tested, the measured electrical admittances perfectly agreeing with theoretical predictions. As in the case of classical Lamb waves, the fundamental mode was found almost insensitive to the wafer thickness. The frequency control then is achieved by the poling period, whereas the excitation principle coincides with the one of FBARs and hence allows for improved power handling capabilities regarding standard SAW transducers.

These experiments were followed by the fabrication of PPT-based wave-guides. One more time, technology advances allowing for room-temperature reliable bonding of heterogeneous material based on metal-metal compression and lapping/polishing operations (Gachon et al, 2008), PPTs built on single crystal $LiNbO_3$ Z-cut layers were bounded atop Silicon and lapped down to a few tens of µm to develop RF passive devices compatible with silicon-based technologies (Courjon et al, 2008). Once again, a good agreement between theory and experiments was emphasized. Two main contributions to the electrical admittance of the test devices were identified as an elliptical mode and a longitudinal propagation radiating in the substrate. The first mode was found again low sensitive to the $LiNbO_3$ thickness and the technological achievement proved the feasibility of thinned-$LiNbO_3$-layer-based PPT/Silicon devices.

These results were sufficiently convincing for pushing ahead the investigations toward even more complicated structures. An innovative solution then was proposed to address' the need for spectral purity, immunity to parasites, simple packaging and fabrication robustness (Bassignot et al, 2011). The proposed structure is still based on PPT but the later is inserted between two guiding substrates. It was pointed out first theoretically and afterward experimentally that a wave could propagate without any acoustic losses and decreases exponentially in such a structure (definition of a guided mode). This description is close to the one of interface waves (Kando et al, 2006) and fairly coincides with the behavior of isolated wave (Elmazria et al, 2009). In the proposed approach however, two metal-metal bonding are required and naturally provide the excitation electrodes, yielding a significant simplification of the device fabrication compared to classical IDT-based devices. One more time, theory and experiments were according well, and the implementation of such a waveguide for the fabrication of a one-port resonator has been demonstrated (Bassignot et al, 2011). This resonator was used to stabilize a Colpitts oscillator, allowing for stability measurements. Another convincing application was demonstrated by Murata (Kadota et al, 2009) for a RF filter operating at a quite low frequency but exhibiting a double mode transfer function yielding sharp transition bands, a rejection of about 20 dB with small insertion losses (less than 5 dB). Although not accurately explained in the above-referred text, one can actually guess that the filter operation is based on mode coupling as the filter architecture does not leave any possibility for other operation principles.

In this chapter, some fundamental elements are reported to understand the transducer operation. Theoretical analysis results and theory/experiment assessments are shown, allowing to illustrate the level of control for designing actual devices based on that principle. Technological aspects concerning the poling operations as well as bonding and

lapping/polishing techniques are briefly reminded. The fabrication and test of more complicated waveguides are then described and finally the use of Si/PPT/Si resonators for oscillator purposes is presented. As a conclusion, further developments needed to widen to more applications (such as filters or even sensors) are discussed, pointing out the advantages of the principle but also the points for each more investigations are still needed.

2. Basic principle of PPTs

The Periodically Poled Transducer is fundamentally based on a periodically poled piezoelectric medium (see Fig.1). Each side of this medium is metalized in order to obtain a capacitive dipole in which elastic waves can be excited by phase construction. Such a periodically poled structure can be advantageously achieved on ferroelectric materials like PZT thanks to the rather small value of its coercive electric field (the absolute value of the electric field above which the spontaneous polarization can be inverted) or $LiNbO_3$ and $LiTaO_3$. It advantageously compares to standard surface acoustic wave (SAW) devices considering its natural operation, yielding a factor of two for the working frequency as it exploits a second harmonic condition (contrarily to SAW which operates at Bragg frequency). Also it exhibits an advantage compared to film bulk acoustic resonator (FBAR) as the periodicity controls the operation frequency (and not only the plate thickness as for FBAR).
As mentioned in introduction, the first mode of most PPT-based device is low sensitive to the ferroelectrics plate thickness and therefore the solution reveals more robust than bulk wave devices considering frequency control. An intuitive analysis of the device operation yields the conclusion that only symmetrical modes can be excited in plates exhibiting geometrical symmetry. This consideration of course fails as soon as the PPT is bonded on a substrate, but it still holds for Si/PPT/Si structure.

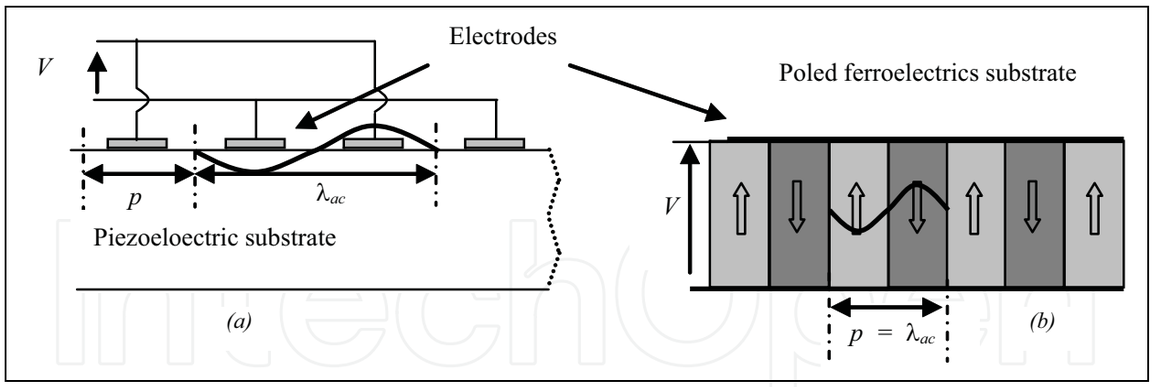

Fig. 1. Comparison between principles of standard SAW devices (a) and poled ferroelectric film transducers (b)

Whatever, the simulation of PPT cannot be achieved using simple harmonic models or even Green's function analysis. Even if analytical efforts have been initially achieved to predict PPT efficiency, the use of finite element analysis has revealed particularly advantageous and much more flexible than plane-wave expansion approaches for instance (Wilm et al, 2002). Furthermore, for estimating guiding capabilities of PPT bonded on substrates, the combination of finite element and boundary element achieved for passivated SAW devices (Ballandras et al, 2009) or interface waves (Gachon et al, 2010) is ideally suited.

3. Technological developments

3.1 Periodic poling of ferroelectrics single crystal

As mentioned above, the poling process can be rather easily applied to PZT for which the coercitive field is small enough to allow for an efficient control of the domain polarity. In the case of lithium niobate or tantalate, this situation is quite different because of the large value of their coercitive fields (21 $MV.m^{-1}$ compared to 2.5 $MV.m^{-1}$ max. for PZT). As a consequence, the development of a dedicated poling bench was required to control the poling of thick (500µm) Z-cut $LiNbO_3$ and $LiTaO_3$ plates. This is detailed in ref (Courjon et al, 2007). Consequently, only a brief description of the bench principle is reported here. The poling bench mainly consists of a high voltage amplifier used to submit the ferroelectrics wafer to an electric field strong enough to invert its native polarization. To achieve such an operation, one needs the use of optical grade Z-cut plates. Wafers are cut in the same boule to well control the poling conditions. A photoresist mask is achieved atop one wafer surface, which defines the poling location. A lithium chloride electrolyte is used to ensure good electric contacts with the wafer surfaces. A dynamic poling sequence then is imposed to the wafer, progressively reaching the expected coercitive field. An evidence of successful poling is obtained by measuring the current of the whole electrical system. Once evidence of transient current obtained, the device is considered to be poled. Following this sequence, and providing no short circuit occurs, an almost perfect poling can be achieved. Figure 2 shows a principle scheme of the poling bench.

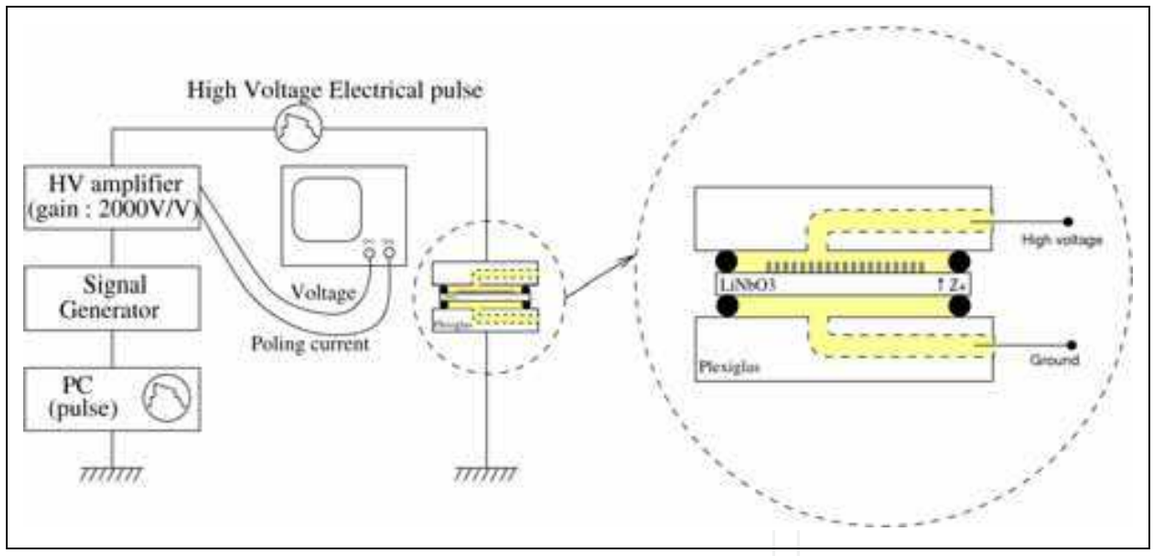

Fig. 2. Scheme of the poling bench used to fabricate periodically poled ferroelectric plates

Our experiments have been achieved on thick (500 µm) optical quality Z-cut $LiNbO_3$ plates from CTI (CA, USA) and on Z-cut LiTaO3 plates from Redoptronics (CA, USA). Consequently, the voltage needed to invert the domains is approximately 11kV. The domains to be poled have been defined using a photo-resist pattern on one plate surface with poling periods (i.e. acoustic wavelengths) ranging from 50 to 5 µm (corresponding to 2.5 and 25 µm line-width respectively). The plate is held in a plexiglas (PMMA) mounting by means of two O-ring which create two cavities fulfilled by the saturated lithium chloride solution used as a liquid electrode (as it is shown in the scheme of fig.2).

The high poling voltage is applied to the plate following the sequence established by Myers et al. (Myers et al, 1995). This sequence is designed to favor the domain nucleation, to stabilize the inverted domains (i.e. to avoid back-switching of the domains) and to avoid electrical breakdowns. The poling process is monitored by measuring the electric current crossing the wafer during the sequence. The signature of a successful domain inversion corresponds to a voltage dropping, due to the high voltage amplifier saturation, while a current discharge occurs simultaneously. The poling can be easily controlled by a simple optical post-observation, as it generates a contrast between at the edge of the poled domains. We have emphasized that although the $LiNbO_3$ poling was quicker and simpler than the $LiTaO_3$ one, the later was more controllable once increasing the stabilization delay. Figs 3 & 4 show normalized electrical pulse and example of successful poling for both materials.

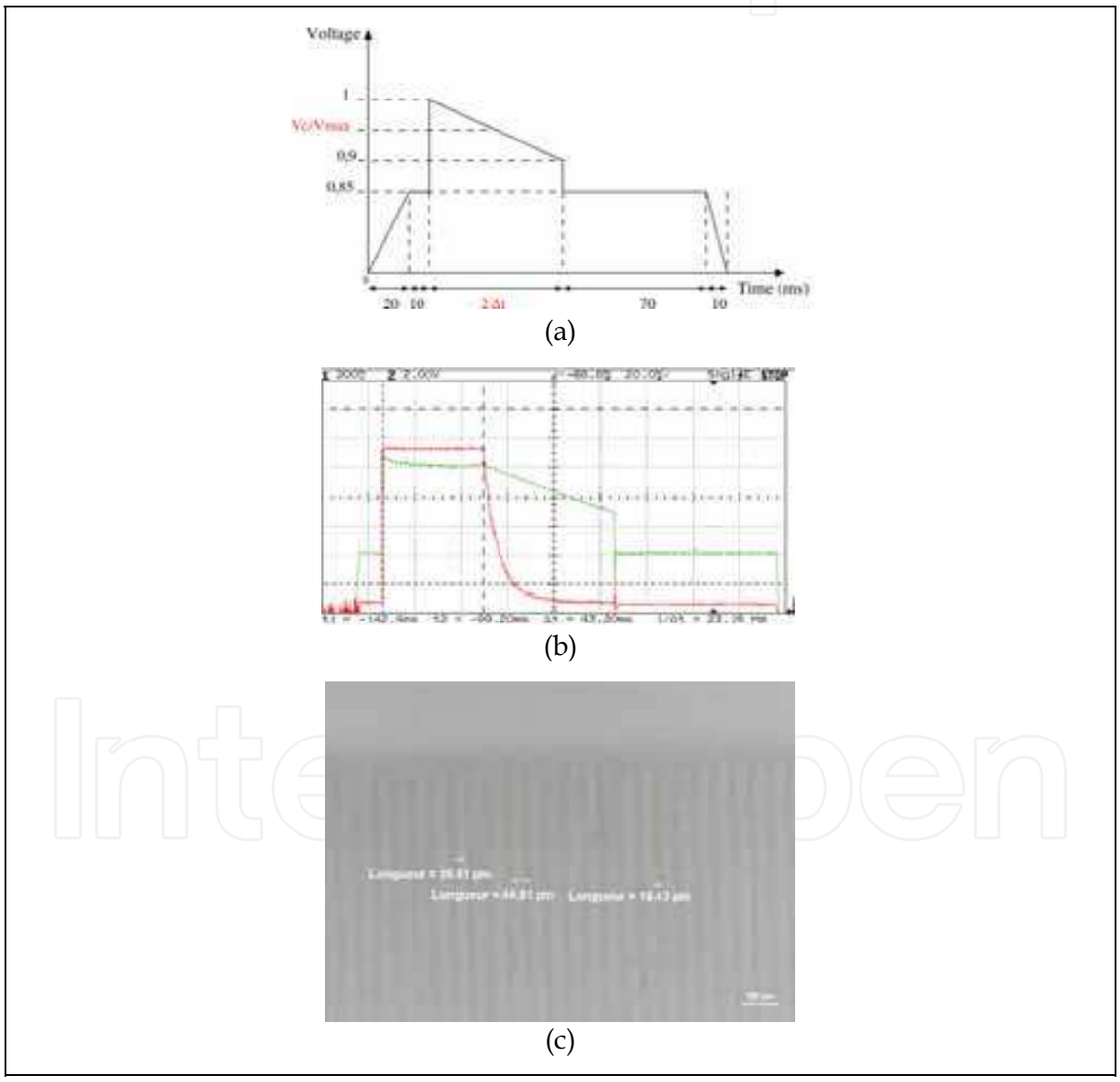

(a)

(b)

(c)

Fig. 3. (a) Normalized electrical pulse for the $LiNbO_3$ poling, (b) Electrical potential (green) and current (red) provided by the amplifier to the poling circuit (c) Optical microscope observation of a periodically poled lithium niobate substrate

We have tested various configurations of Lamb-wave PPTs, the simplest configuration using the periodic poling approach just consisting in depositing electrodes on both side of the poled plate. Both practical implementation and simulations have been developed, based on the above-described approach and on finite element analysis for the later. Figure 5 shows that an excellent control of such device and an accurate description of its operation can be achieved.

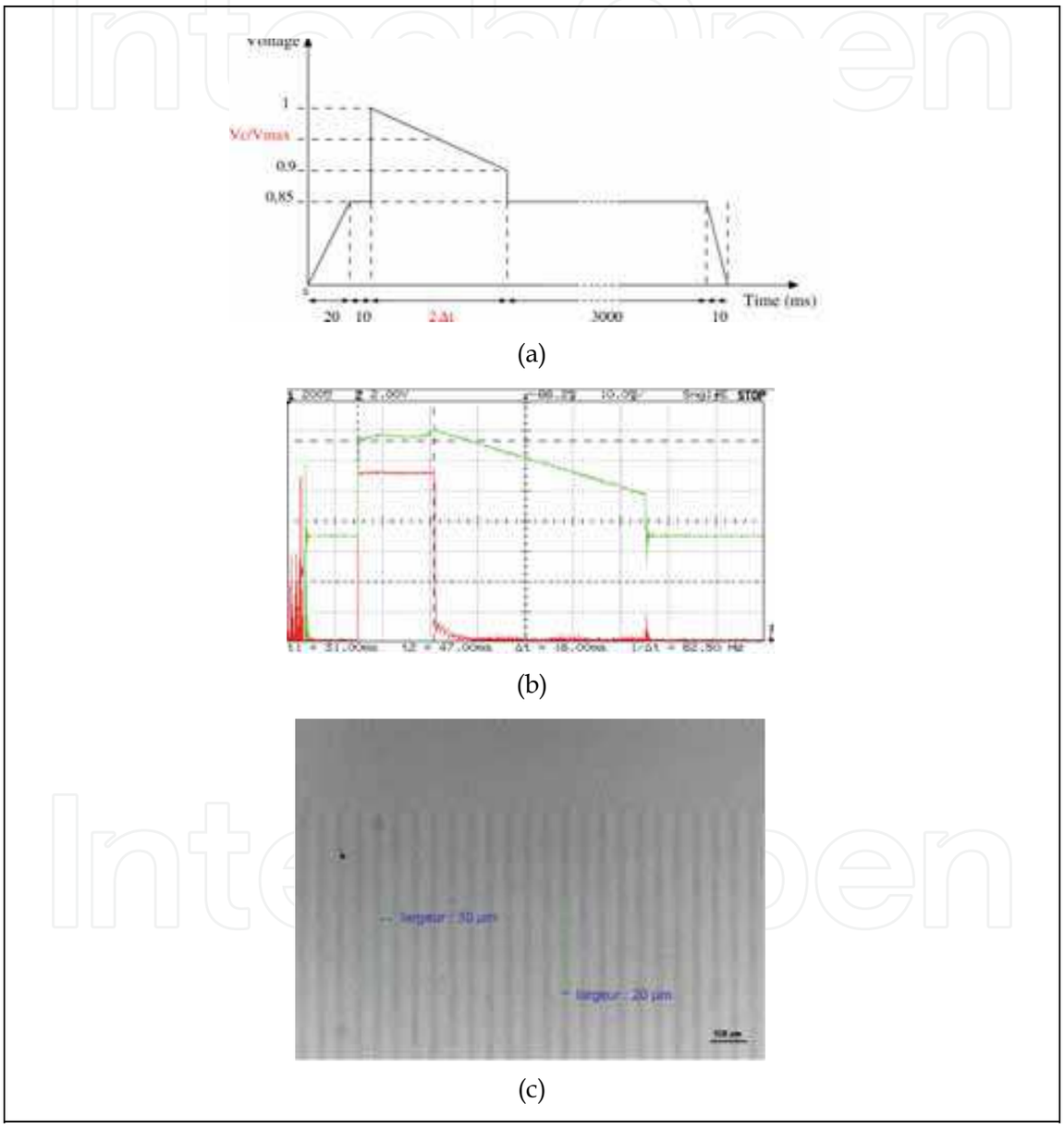

Fig. 4. (a) Normalized electrical pulse for the $LiTaO_3$ poling, (a) Electrical potential (green) and current (red) provided by the amplifier to the poling circuit (b) Optical microscope observation of a periodically poled lithium niobate substrate

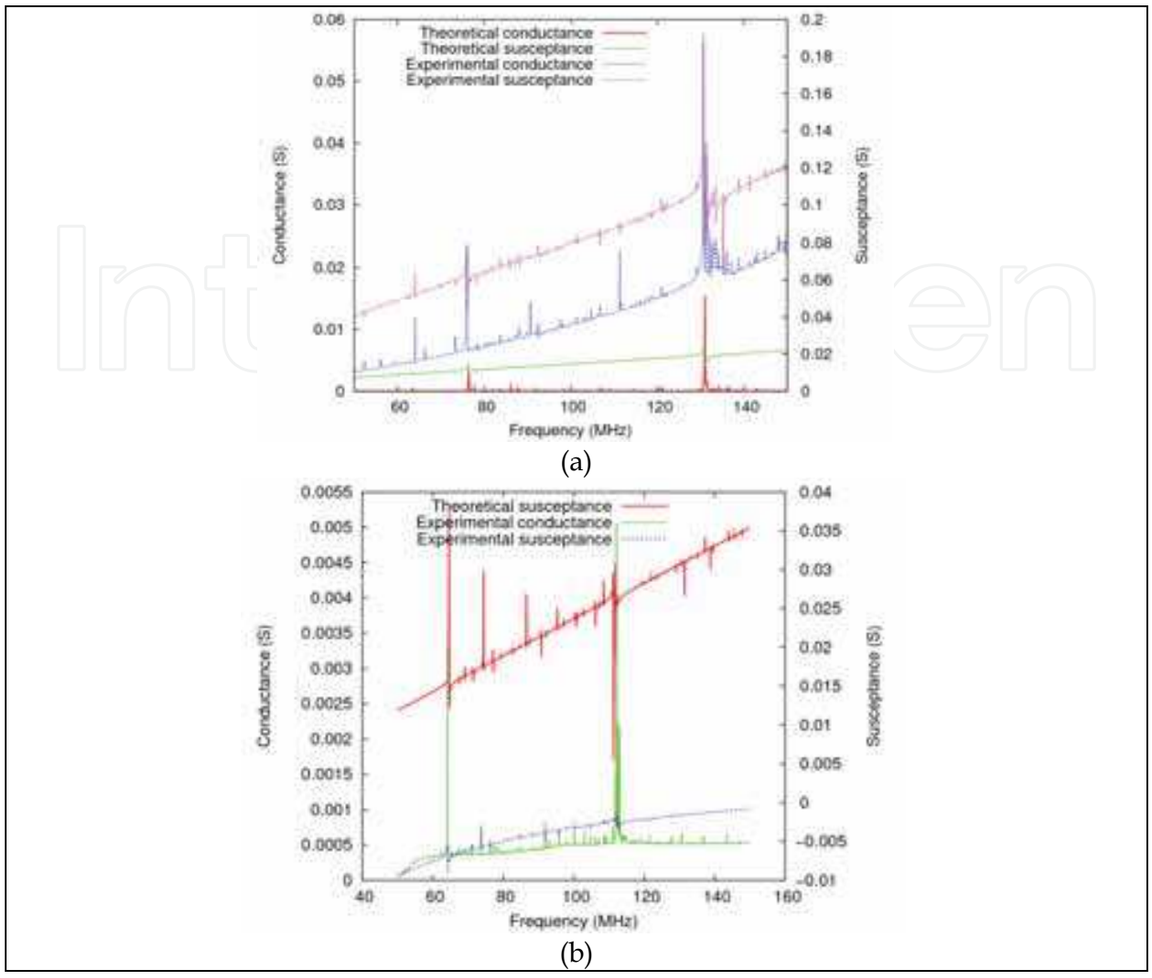

Fig. 5. Theory/experiment assessment for a Lamb wave multi-mode device with 50µm of poling period built on a Z-cut $LiNbO_3$ plate (a) and a Z-cut $LiTaO_3$ plate (b)

3.2 Wafer bonding and lapping/polishing of ferroelectrics upper-layer

The process is based on the bonding of two single-crystal wafers. In this approach, optical quality polished surfaces are mandatory to favor the wafer bonding. A Chromium and Gold thin layer deposition is first achieved by sputtering on both ferroelectrics ($LiNbO_3$ or $LiTaO_3$) and Silicon wafers. Both wafers then are pre-bonded by a mechanical compression of their metalized surfaces into an EVG wafer bonding machine as shown in Fig.6. During this process, we heat the material stack at a temperature of 30°C and we apply a pressure of 65N.cm^{-2} to the whole contact surface. The bonding can be particularly controlled by adjusting the process duration and various parameters such as the applied pressure, the process temperature, the quality of the vacuum during the process, etc. We actually restrict the process temperature near a value close to the final thermal conditions seen by the device in operation. Since Silicon and ferroelectrics materials have different thermal expansion coefficients, one must account for differential thermo-elastic stresses when bonding both wafers and minimize them as much as possible. A variant to this process has been tested recently, based on the use of a megasonic cleaning pre-bonder, allowing to significantly reduce the number of bonding defects. Once the pre-bonding achieved, we finish the

bonding process by applying a strong pressure to the stack which eliminates most of the bonding defects not due to dusts and organic impurities (the later being eliminated by the megasonic cleaning), yielding 90% bonded surface and even more.

Fig. 6. Wafer bonding: EVG bonding machine used for wafer pre-bonding (the bonding is finished using a classical press)

Once the bonding achieved, it is necessary to characterize the adhesion quality. Due to the thickness of the wafers and the opacity of the stack (metal layers, Silicon), optical measurements are poorly practicable. As we want to avoid destructive controls of the material stack, ultrasonic techniques have been particularly considered here. The reliability of the bonding then is analyzed by ultrasonic transmission in a liquid environment. The bonded wafers are immersed in a water tank and the whole wafer stack surface is scanned. Fig. 7 presents a photography of the bench. Two focalized transducers are used as acoustic emitter and receiver. They are manufactured by SONAXIS with a central frequency close to 15 MHz, a 19mm active diameter and a 30mm focal length. The beam diameter at focal distance at -6dB is about 200µm. Finally Fig.8 shows an example of bonding characterization. One can see that the bonding is homogeneous and presents few defects. The surface can be considered as bonded (and specially the area of the PPT one can hardly distinguish).

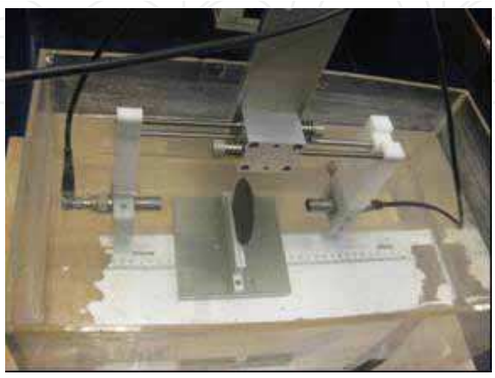

Fig. 7. Ultrasonic tank for bonding characterization based on acoustic transmission (any defect in the path of the ultrasonics beam scatters the pressure wave)

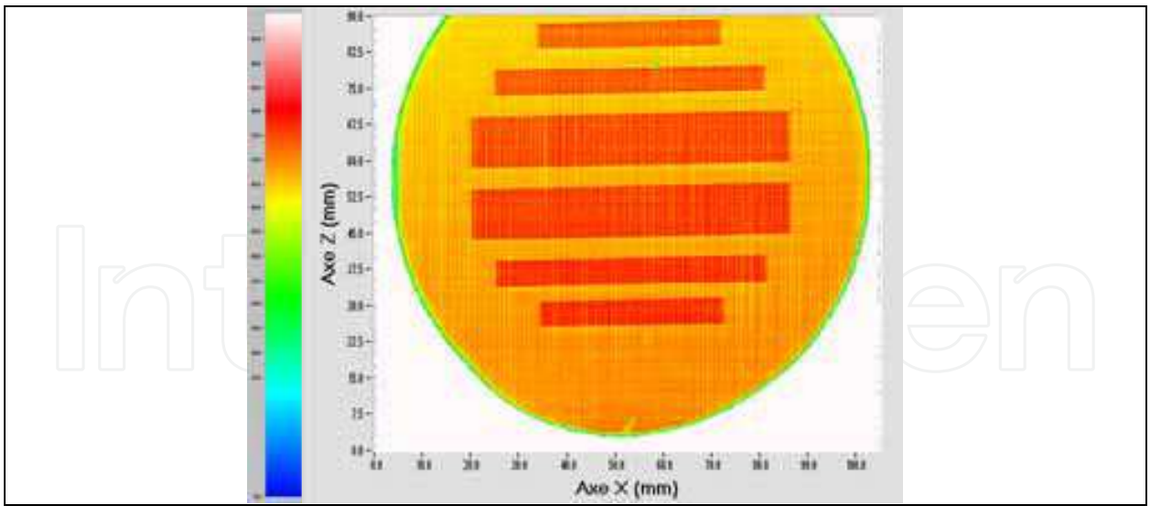

Fig. 8. Example of Si/Lithium niobate bonded surface (4-inch wafers), characterized using ultrasound transmission (Fig. 7)

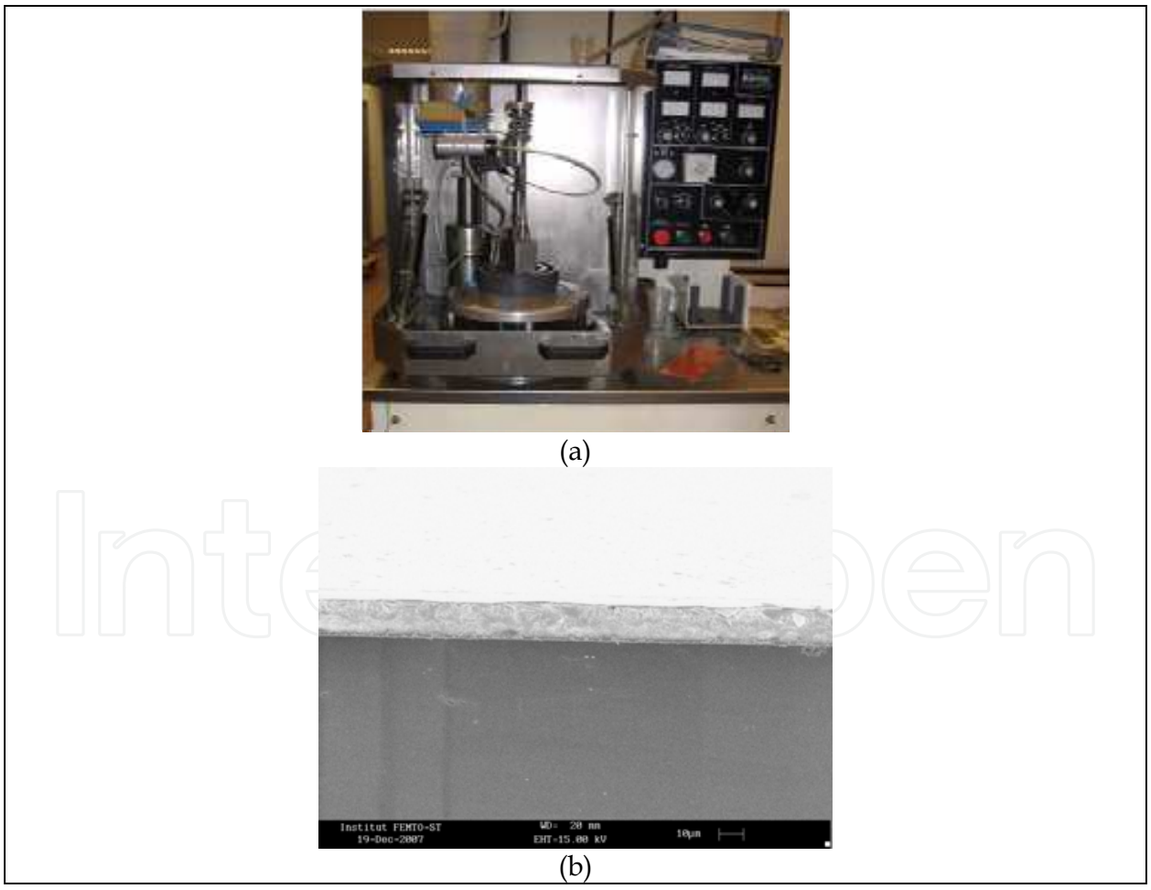

(a)

(b)

Fig. 9. Photograph of the SOMOS equipment used for lapping/.polishing operations (a) and SEM view of a lithium niobate wafer bonded on a silicon wafer and finally lapped down to about 10µm (b)

The piezoelectric wafer is subsequently thinned by a lapping step to an overall thickness of 100 microns. The lapping machine used in that purpose and shown in fig.9 is a SOMOS double side lapping/polishing machine based on a planetary motion of the wafers (up to 4" diameter) to promote abrasion homogeneity. We use an abrasive solution of silicon carbide. We can control the speed of the lapping by choosing the speed of rotation, the load on the wafer, the rate of flow or the concentration of the abrasive. It is then followed by a micro-polishing step. This step uses similar equipment dedicated to polishing operation and hence using abrasive solution with smaller grain. Fig. 9 shows the equipment used to lap and polish the piezoelectric material and an example of a $LiNbO_3$ layer thinned down to a few tenth of microns, bonded on Silicon.

4. PPT/Si wave-guides

Therefore, waveguides based on a thinned $LiNbO_3$ or $LiTaO_3$ plate bounded on Silicon have been implemented along the flow chart of fig.10, taking advantage of the acoustic velocities in silicon higher than in the above-mentioned materials to meet the guiding conditions. Here again (as shown in fig.11), the accordance between experimental measurements and theoretical predictions confirms the control of the device operation and allows for developing design process.

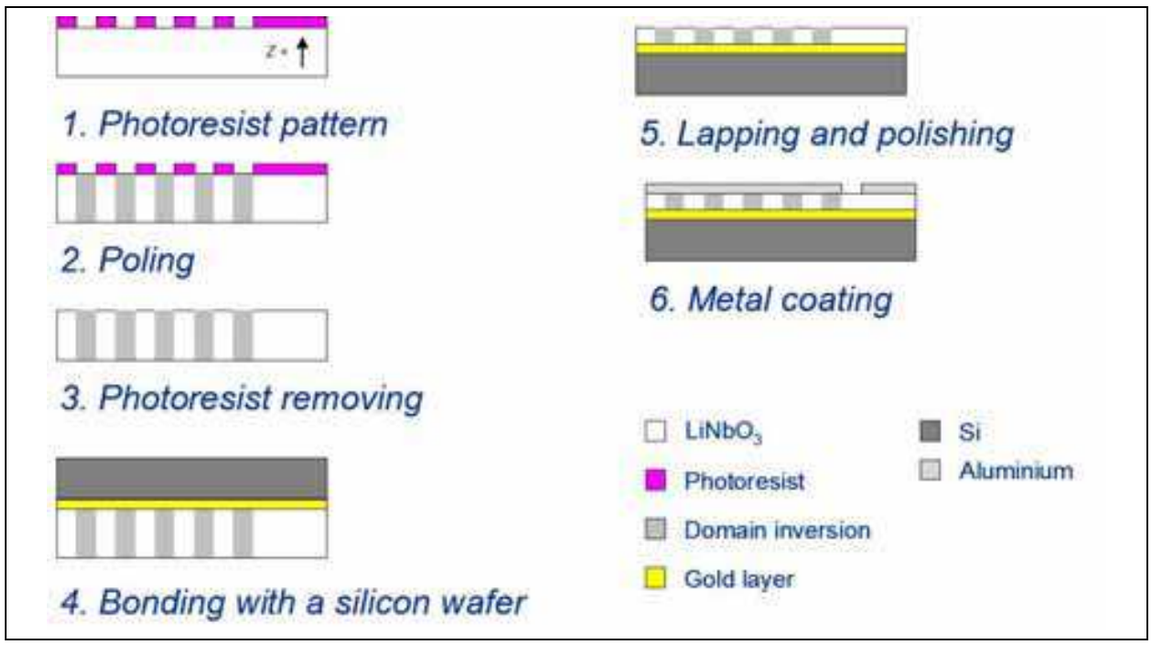

Fig. 10. Flow chart of the fabrication of PPT/Si waveguide

Fig. 12 presents another comparison between measured responses of the implemented devices and the theoretical harmonic admittances obtained with our periodic finite element code. The $LiNbO_3$ layer thickness has been measured for the devices, allowing for accurate computations based on realistic parameters. Here are the results for the 40µm period devices. Since the implemented single-port test devices are quite long and almost behave as single port resonators, the comparison between measurement and harmonic admittance results makes sense.

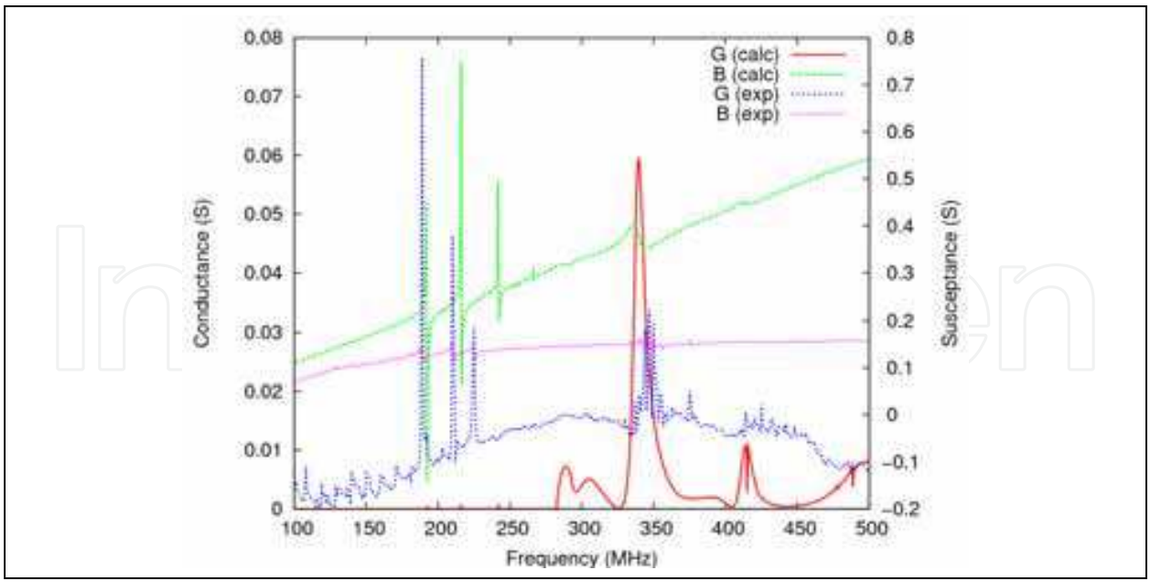

Fig. 11. Theory/experiment comparison for a 20µm period PPT on Silicon ($LiNbO_3$ thickness = 26µm)

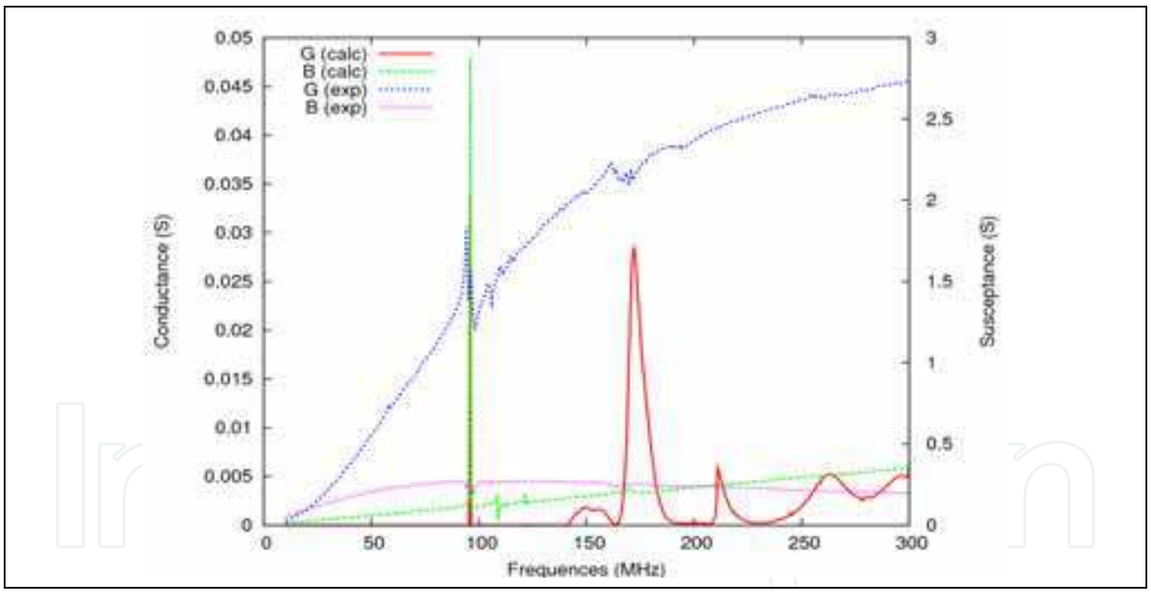

Fig. 12. Theory/experiment assessment for a 40 µm period PPT ($LiNbO_3$ thickness = 50 µm)

5. Si/PPT/SI-based waveguide, resonator and oscillator

Finally, we have developed an isolated wave guide allowing for the propagation of acoustic waves within a PPT plate in between two silicon substrates, yielding advanced packaging opportunities. Fig. 13 illustrates this configuration and Fig.14 shows the kind of theoretical prediction one can obtained using FEM/BEM harmonic computations to demonstrate the targeted guiding effect.

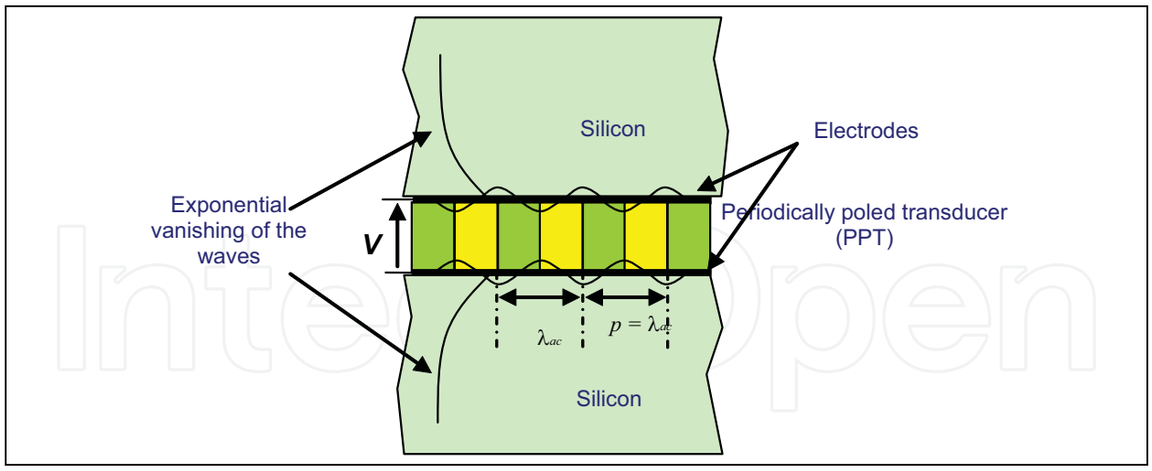

Fig. 13. Principle of the PPT isolated wave transducer

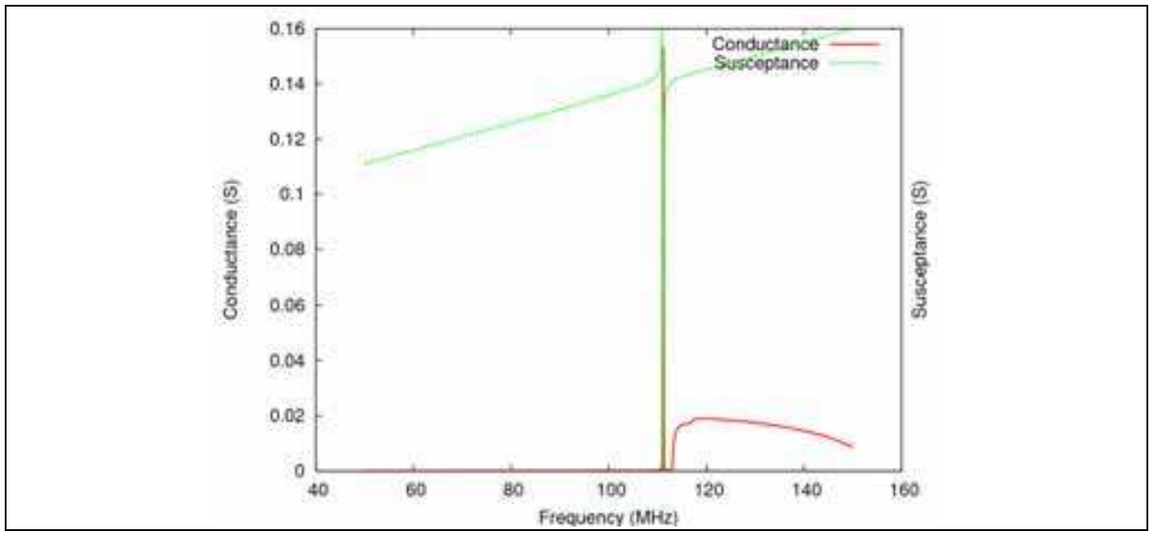

Fig. 14. Example of harmonic admittance computed for a Si/$LiNbO_3$/Si transducer/waveguide, the period of the PPT (wavelength) is 50µm, the niobate layer is 30µm thick (the pole is the signature of a guided mode).

The fabrication of acoustic waveguides based on PPTs consists in bonding a silicon wafer on each side of the periodically poled wafer, as described in fig. 15. In that purpose, the 500 µm thick Z cut lithium niobate wafer is poled and bonded on a (100) 3" doped silicon wafer using a wafer bonding technique developed in our group based on a metal-metal adhesion at room temperature promoted by a high pressure applied to the material stack (Fig.15). The study of the dispersion properties enables to define a specific configuration using a thinned PPT layer of about 30 µm. The $LiNbO_3$ wafer thinning is achieved by home-made lapping and polishing techniques. After this step, the stack of Si(380 µm)/$LiNbO_3$(20 µm) is bonded again on a doped silicon wafer with the same properties that the first one (Fig.16). Several devices have been built along this approach but we mainly have focused our attention on thicker structures (using 500µm thick lithium niobate wafers) for characterization and application purposes.

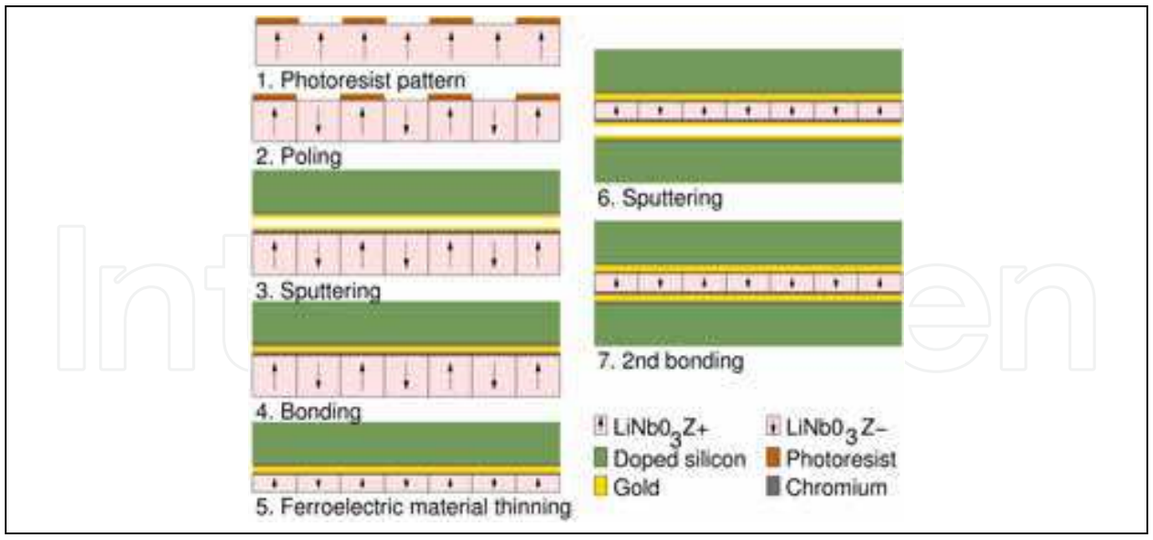

Fig. 15. Flowchart which summarizes the different steps of fabrication

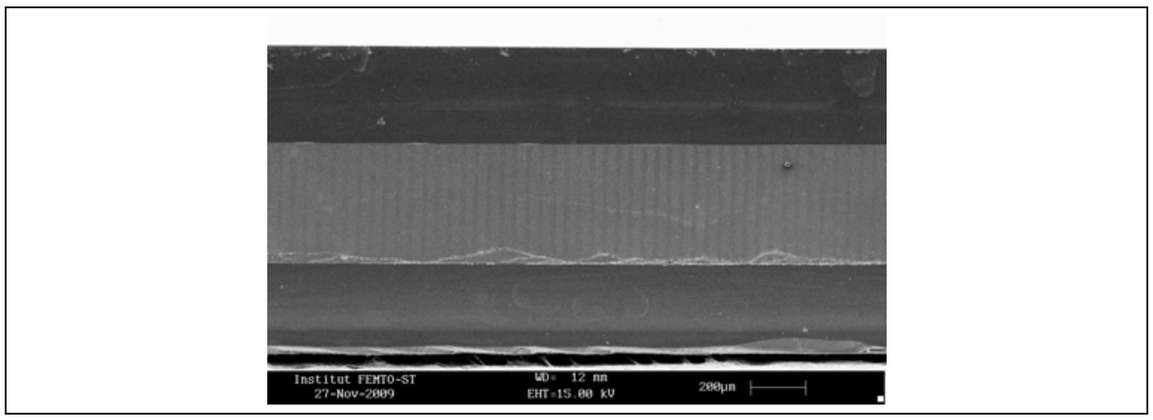

Fig. 16. SEM view of a Si/PPT/SI transducer, clearly showing the periodic poling of the transducer

Operational test vehicles have been achieved using doped silicon wafers to ease the electrical contact. The transducer was built in lithium niobate with a 50 µm period and a thickness equal to 500 µm. Theoretical and measured electrical admittances agree well and allow for identifying a main contribution corresponding to a guided longitudinal mode at 131 MHz (fig. 17). The corresponding phase velocity is very close to the one of the PPT alone (i.e. 6500 $m.s^{-1}$). The elliptically polarized mode excited using the PPT alone and exhibiting a phase velocity of about 3800 $m.s^{-1}$ is not excited nor guided in this configuration. This mode actually needs a free surface to satisfy its boundary conditions (similarly to a Rayleigh wave) and therefore, the existence of rigid boundary conditions on each side of the PPT prevents its excitation and propagation.

This resonator operating near 131 MHz exhibits a quality factor of 13000 and an electromechanical coupling k_s^2 equal to 0.25 % (twice higher than the one of a SAW resonator on Quartz). The corresponding phase rotation (320°) and the dynamic of its electrical reflection coefficient (S_{11}=-8 dB) are suitable for oscillator applications. Such a device therefore has been built using a negative resistance scheme (the so-called Colpitts circuit [Colpitts]).

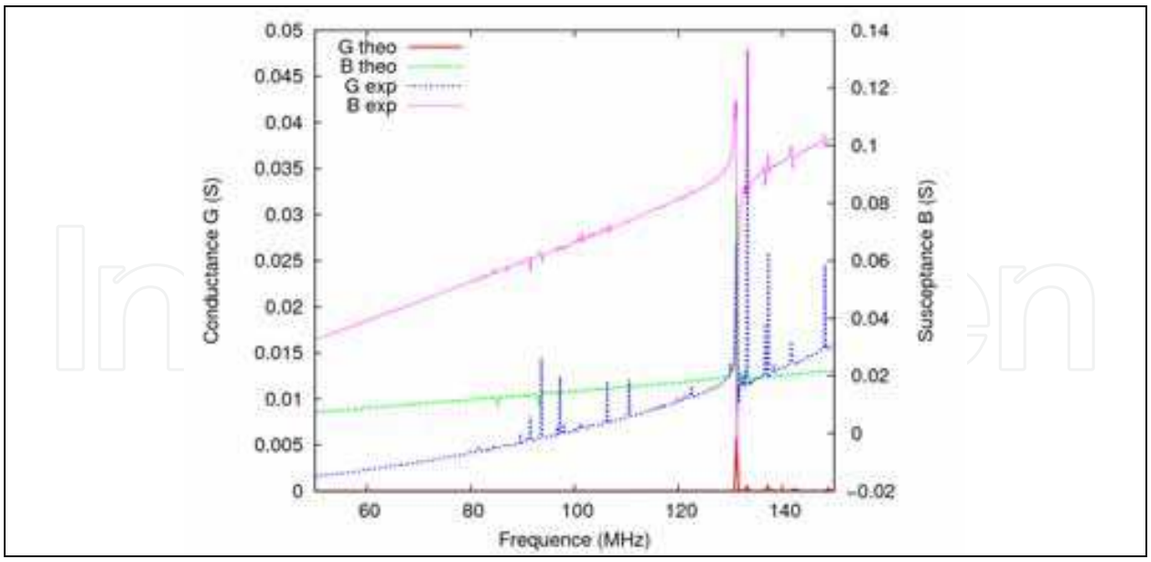

Fig. 17. Theoretical and experimental admittances of a Si(380µm)/$LiNbO_3$(500µm) PPT/Si(380µm) sandwich

A specific printed circuit has been built in that matter (Fig.18). Note that thanks to the isolation of the mode, one could glue the resonator directly on the board allowing for easily grounding the device. A single gold wire then is used to connect the resonator to the oscillator (such a connection yields a notable sensitivity to RF parasites and hence will be improved in the next future). The phase noise of the oscillator at 100 kHz from the carrier shows a value less than -160 dBc/Hz, which can be honestly compared with other acoustic wave oscillators at such frequency, accounting for the fact that the device was excited with a quite low signal level (-6dBm). Therefore, increasing the excitation should allow for a significant reduction of the noise floor and then advantageously compete with standard solutions. Moreover, as the wave guide appears really robust concerning packaging and back end conditioning, it can be integrated more easily than any other acoustic wave based solutions and benefit from a clear applicative potential.

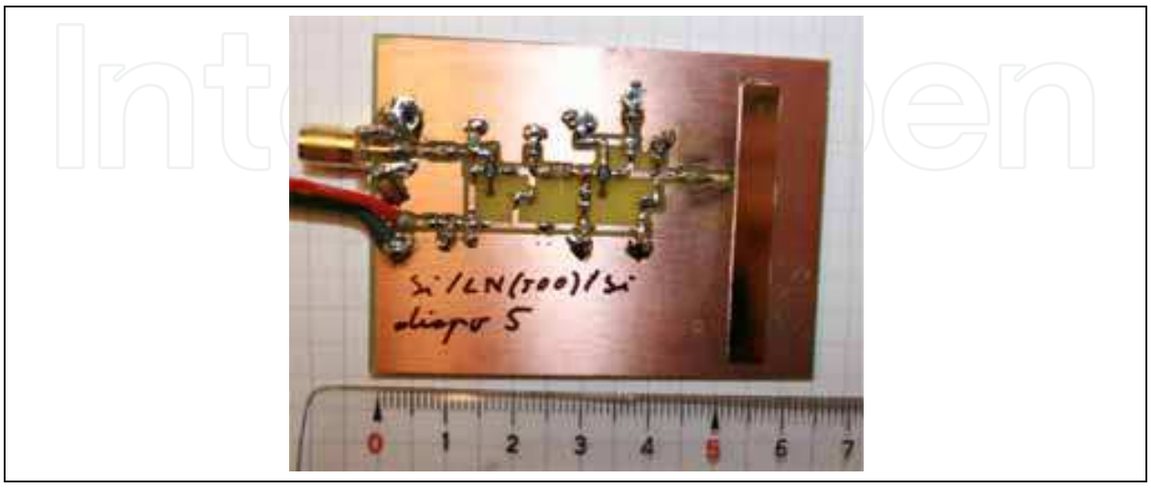

Fig. 18. The oscillator board implemented for phase noise tests

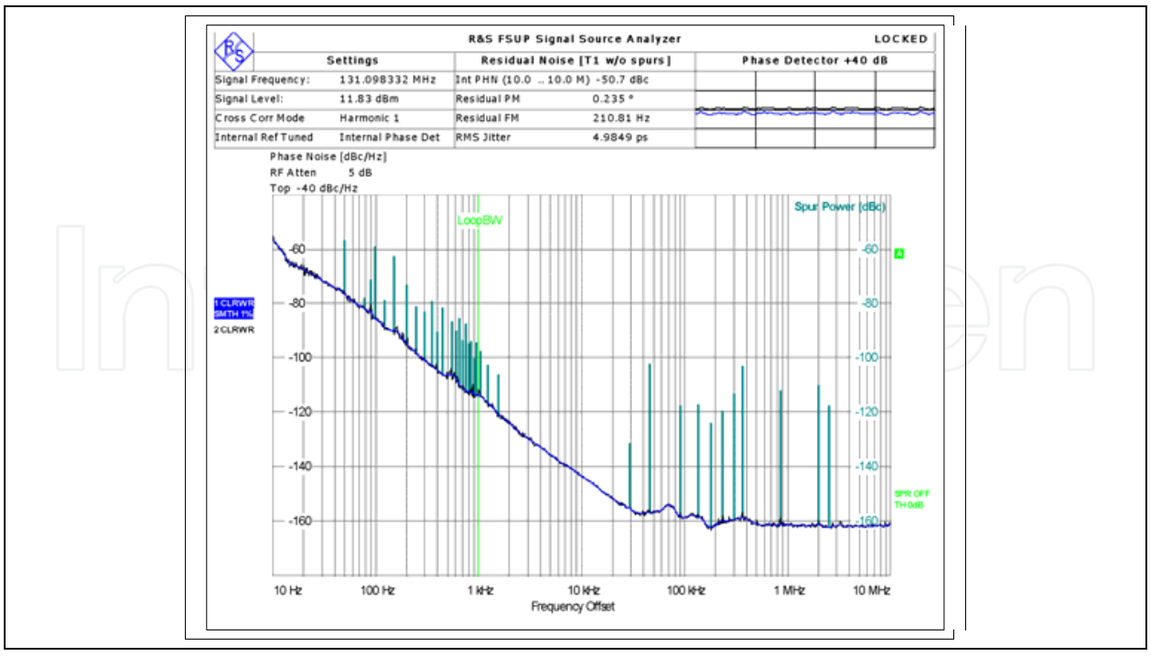

Fig. 19. Phase noise of the 131 MHz oscillator stabilized with a Si/PPt/Si resonator. The noise floor is better than -160 dBc/Hz.

6. Conclusion

In this chapter, we have discussed the standard techniques implemented for optimizing PPTs for fabricating test vehicles and we have proposed a detailed analysis of the experimental tests. We propose some guidelines for future developments and implementation of these new waveguide principles to answer the requirements for the next generation of passive signal processing components, and more particularly resonators and filters. However, because of its very particular configuration, the Si/PPT/Si structure is considered as a potential candidate for sensor applications, particularly when the sensor is expected to be inserted in hosting bodies submitted to parametric perturbations such as stress, vibration or pressure. In that case, the device can be connected directly to the proof body without the need to protect any surface, providing therefore more robustness than SAWs or even bulk-wave-based sensors.

7. Acknowledgment

This work has been achieved in the Dominos program framework, funded by the European Community as the InterReg project DOMINOS and was also funded by the french DGA (Délégation Générale pour l'Armement) under grant #07-34-020.

8. References

S. Ballandras et al, (2003); A novel surface wave transducer based on periodically poled piezoelectric domain, Frequency Control Symposium and PDA Exhibition Jointly with the 17th European Frequency and Time Forum, 2003. Proceedings of the 2003 IEEE International, vol., no., pp. 893- 896

S. Ballandras et al., (2009) A mixed finite element/boundary element approach to simulate complex guided elastic wave periodic transducers. Journal of Applied Physics 105 1 014911

F. Bassignot et al, (2011) A New Acoustic Resonator Concept Based on Acoustic Waveguides Using Silicon/Periodically Poled Transducer/Silicon Structures for RF Applications, IEEE IFCS, San Francisco

P. Bradley et al, (2000), "Film bulk acoustic resonator (FBAR) duplexer"-- U.S. Patent (USP) #6262637; Agilent inventors Paul Bradley, John Larson, Richard Ruby).

E. Courjon et al, (2007) Lamb wave transducers built on periodically poled Z-cut LiNbO3 wafers, Journal of Applied Physics, 102, 114107

E. Courjon et al, (2008) Characterization of guided modes excited by periodically poled transducers on Si," Frequency Control Symposium, 2008 IEEE International , vol., no., pp.604-608

O. Elmazria et al, (2009), AlN/ZnO/diamond structure combining isolated and surface acoustic waves, Applied Physics Letters, vol.95, no.23, pp.233503-233503-3

D. Gachon et al, (2008) Fabrication of High, Frequency Bulk Acoustic Wave Resonator Using Thinned Single−Crystal Lithium Niobate Layers, Ferroelectrics, Vol.362, n°1, pp. 30−40

D. Gachon et al. (2010) Prediction and Measurement of Boundary Waves at the Interface Between LiNbO3 and Silicon. IEEE Transactions on Ultrasonics Ferroelectrics and Frequency Control57 7 1655−1663

J.A. Greer et al, (1990) Metalllisations for Surface Acoustic Wave Resonators: film properties and device characteristics, Proc. of the IEEE Ultrasonics Symposium, Vol.1, pp.483-491

G.F. Iriarte et al, (2003) SAW COM parameter extraction in AlN/diamond layered structures, IEEE Trans. on UFFC, Vol. 50, N°11, pp. 1142–1547

K. Higaki et al, (1997) High power durability of diamond surface acoustic wave filter, Ultrasonics, Ferroelectrics and Frequency Control, IEEE Transactions on , vol.44, no.6, pp.1395-1400

M. Kadota et al, (2009) Acoustic Wave Devices using Periodical Poled Z-cut $LiTaO_3$ Plate, Proc. of the joint IEEE IFCS-EFTF, Besançon, pp919-922, 2009

H. Kando et al (2006) 6B-4 RF Filter using Boundary Acoustic Wave, Ultrasonics Symposium, IEEE, vol., no., pp.188-191

R. Lanz, P. Muralt, (2005) Band pass filters for 8 GHz using solidly mounted Bulk Acoustic Wave Resonators, IEEE Trans. on UFFC, Vol. 52, N°6, pp. 946–946

K.M. Lakin, (2003) "Thin film resonator technology", Proc. of the joint IEEE IFCS-EFTF, pp. 1-14

D.P. Morgan, (1985) Surface Wave Devices for Signal processing, Studies in Electrical Eng. 19, Elsevier Ed.

L. E. Myers et al, (1995) Quasi-phase-matched optical parametric oscillator", JOSA B, Vol. 12, Issue 11, pp. 2102-2116

R. Salut & al, (2010) Fabrication of GHz Range Oscillators Stabilized by Nano-Carbon-Diamond-Based Surfcae Acoustic Resonators, Proc of the IEEE International Ultrasonics Symposium, San Diego

A. K. Sarin Kumar et al (2004), High-frequency surface acoustic wave device based on thin-film piezoelectric interdigital transducers, Appl. Phys. Lett. 85, 1757 doi:10.1063/1.1787897 (*3 pages*)

M. Wilm et al, (2002) A full 3D plane-wave-expansion model of 1-3 piezoelectric composite structures, J. Acoust. Soc. Am., vol. 112, n°3, pp. 943-952

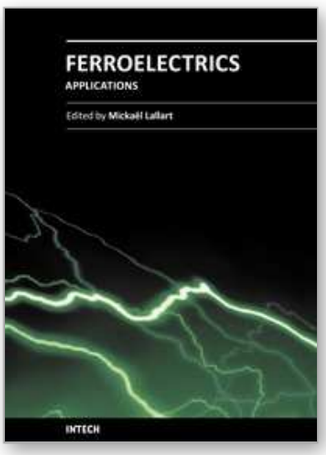

Ferroelectrics - Applications
Edited by Dr. MickaÃ«l Lallart

ISBN 978-953-307-456-6
Hard cover, 250 pages
Publisher InTech
Published online 23, August, 2011
Published in print edition August, 2011

Ferroelectric materials have been and still are widely used in many applications, that have moved from sonar towards breakthrough technologies such as memories or optical devices. This book is a part of a four volume collection (covering material aspects, physical effects, characterization and modeling, and applications) and focuses on the application of ferroelectric devices to innovative systems. In particular, the use of these materials as varying capacitors, gyroscope, acoustics sensors and actuators, microgenerators and memory devices will be exposed, providing an up-to-date review of recent scientific findings and recent advances in the field of ferroelectric devices.

InTech Europe
University Campus STeP Ri
Slavka Krautzeka 83/A
51000 Rijeka, Croatia
Phone: +385 (51) 770 447
Fax: +385 (51) 686 166
www.intechopen.com

InTech China
Unit 405, Office Block, Hotel Equatorial Shanghai
No.65, Yan An Road (West), Shanghai, 200040, China
中国上海市延安西路65号上海国际贵都大饭店办公楼405单元
Phone: +86-21-62489820
Fax: +86-21-62489821

IntechOpen